NO adsorption on fresh and aged Pd-Rh Natural Gas Vehicle catalysts : A TAP approach

Pascal Granger, Y. Renème, Fabien Dhainaut, Yves Schuurman, C. Mirodatos

NO Adsorption and Reaction on Aged Pd–Rh Natural Gas Vehicle
Catalysts: A Combined TAP and Steady-State Kinetic Approach

Pascal Granger
- Y. Renème[1]
- F. Dhainaut[1]
- Y. Schuurman[2]
- C. Mirodatos[2]

Pascal Granger : pascal.granger@univ-lille1.fr
1 Unité de Catalyse et de Chimie du Solide, ENSCL, UMR CNRS 8181, Université Lille 1 Sciences et Technologies, Bât. C3 Villeneuve d'Ascq, 59650 Villeneuve d'Ascq, France
2 Ircelyon, CNRS, Université Lyon 1, 2 avenue A. Einstein, 69000 Lyon, France

Abstract
A combined temporal analysis of products (TAP) and steady-state kinetic study was achieved to characterize the surface reactivity of fresh and aged bimetallic Pd–Rh/Al_2O_3 Natural-Gas Vehicle catalysts.
Single NO pulse TAP experiments were performed on a stabilized surface after exposure to successive NO pulses until to get a steady-state NO conversion. Outlet flow curves recorded during such experiments show fast reaction steps taking place on noble metal particles and a slow process during NO desorption ascribed to the involvement of spill-over effect of chemisorbed NO molecules from the metal to the support. This slow process attenuates on the aged sample likely due to an alteration of the metal/support interface induced by particle sintering at high temperature.
Thermal aging also alters the surface composition of bimetallic Pd–Rh particles which leads to changes in the products distribution from NO dissociation. A similar selectivity behavior is observed from steady-state kinetic measurements during the NO/H_2 reaction. Interestingly, a weak partial pressure dependency of the selectivity reflects a surface Rh enrichment of Pd–Rh particles during aging.

Keywords Thermal aging ; TAP reactor ; NGV Pd–Rh catalyst ; NO adsorption ; $DeNO_x$; N_2O formation
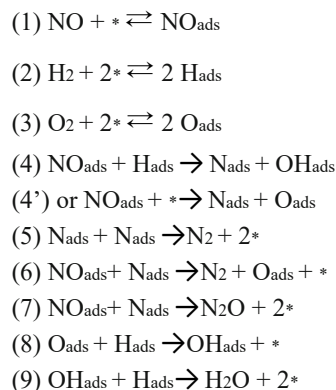
1 Introduction

A growing interest is focused on the development of natural gas fueled-engines [1, 2] due to lower atmospheric pollutant emissions in terms of particulates related to a higher H/C ratio and a better homogeneity of combustion process compared to Diesel engines. Among the different reactions taking place over Natural-Gas-Vehicle (NGV) catalysts, the presence of hydrogen in three-way conditions is of prime importance enhancing the reduction of NO at low temperature typically during the cold start engine [3, 4]. Under three-way conditions, at more elevated temperature, the simultaneous removal of NO_x and methane represents an outstanding issue especially under rich conditions because of the high chemical stability of methane. Since methane is recognized as a greenhouse gas then the efficiency of NGV catalysts implies a complete conversion of unburnt methane at reasonable temperature to preserve the catalyst durability. Up to now, palladium is the most active component to treat methane emissions [5, 6].

Now regarding NO_x removal, Rh is recognized as the most active component to dissociate NO. However, strong NO adsorption on Rh can be detrimental on the catalytic activity and selectivity at low temperature [4, 7, 8] and also at high temperature under three-way conditions when the oxygen coverage becomes significant then preventing NO adsorption and dissociation [9]. In these conditions, the formation of N_2O can occur predominantly. Based on these considerations, the preservation of the metal/support interface could be useful further lowering inhibiting effects due to strong NO or oxygen adsorption. TAP and steadystate kinetic measurements were achieved on aged Pd–Rh/Al_2O_3 to investigate the impact of aging on the adsorptive properties of noble metals and the reactivity of

intermediates. Particular attention was paid to the alteration of the metal/support interface and changes in the surface composition of bimetallic Pd–Rh particles during aging.

Further correlations with steady-state kinetic measurements for the $NO/H_2/O_2$ reaction at low temperature will be tentatively established on the basis of the following reaction mechanism as already suggested over noble metals [4, 10, 11] (Scheme 1).

(1) $NO + * \rightleftarrows NO_{ads}$

(2) $H_2 + 2* \rightleftarrows 2\ H_{ads}$

(3) $O_2 + 2* \rightleftarrows 2\ O_{ads}$

(4) $NO_{ads} + H_{ads} \rightarrow N_{ads} + OH_{ads}$

(4') or $NO_{ads} + * \rightarrow N_{ads} + O_{ads}$

(5) $N_{ads} + N_{ads} \rightarrow N_2 + 2*$

(6) $NO_{ads} + N_{ads} \rightarrow N_2 + O_{ads} + *$

(7) $NO_{ads} + N_{ads} \rightarrow N_2O + 2*$

(8) $O_{ads} + H_{ads} \rightarrow OH_{ads} + *$

(9) $OH_{ads} + H_{ads} \rightarrow H_2O + 2*$

Scheme 1 Mechanism for the reduction of NO by H_2 earlierproposed over noble metals [4, 10, 11]

2 Experimental

Bimetallic Pd and Rh-based catalysts supported on alumina (250 m_2 g_{-1}) was supplied by Umicore containing 2.5 and 0.18 wt % palladium and rhodium respectively [4]. Samples were successively calcined in air at 500 °C for 4 h and then reduced in pure H_2 at 500 °C prior to catalytic reaction.

Thermal aging was performed at 980 °C under controlled atmosphere in the presence of 10 vol% H_2O diluted in air. XPS and IR spectroscopic measurements on fresh and aged $Pd–Rh/Al_2O_3$ catalysts revealed a significant growth of metallic particles and a parallel surface Rh enrichment [12]. Transient measurements were carried out in a TAP-2 set-up at Ircelyon [13]. The catalytic bed was composed of three different zones: 220 mg (or 1 cm long) of quartz, 20 mg (or 0.48 cm) of catalysts and 235 mg of quartz (1.06 cm). The duration between two pulses to return to the baseline varied in the range 1.5–2 s. Each pulse contained 6.0 9 10_{15} molecules of gaseous NO.

Steady-state kinetic measurements were performed at atmospheric pressure in a recycling fixed bed flow reactor with a recycling ratio of 180 to get a CSTR performance.

Outlet gas mixture was analysed by a Balzers quadrupole mass spectrometer and a Hewlett Packard 5890 series II chromatograph fitted with a thermal conductivity detector.

Typically, catalytic measurements were performed with 0.1 g of catalyst, diluted in 0.2 g of a-Al_2O_3, and a global flow rate of 10 L h_{-1}. The catalyst was in powder form with an average grain size of 150 lm. In such conditions it was checked by modifying the catalyst loading at constant space velocity that no significant external diffusion phenomena occurred. The rate of NO conversion and selectivity towards the production of N_2O were calculated according to Eqs. (10) and (11) respectively, where $F_{NO,0}$ was the inlet flow rate of NO, F_i (with $i = N_2$ or N_2O) the outlet flow rates of the products, m the mass of catalyst and X_{NO} the conversion of NO.

3 Results and Discussion

3.1 TAP Response on Aged $Pd–Rh/Al_2O_3$ During Single Pulse Experiments

NO single pulse (SP)-experiments were performed on prereduced catalysts at 400 °C after H_2 exposure. The prereduced samples were then exposed to successive NO pulses at 450 °C till the stabilization of NO conversion corresponding to a steady-state concentration of chemisorbed O atoms at the surface of Pd and Rh atoms coming from NO dissociation. In fact, it was previously verified on the fresh $Pd–Rh/Al_2O_3$ catalyst that the oxygen uptake exceeds that corresponding to the saturation of metallic sites suggesting a significant accumulation of ad-NO_x species on the support [12]. In our temperature conditions (T = 450 °C), partial oxygen desorption can also occur and then releasing a small fraction of vacant sites. This assumption correctly explains experimental data reported in Fig. 1.

As observed, chemisorbed NO molecules can readily dissociate leading to the formation of N_2 and N_2O as primary products. As observed a more extensive production of N_2 takes place on the fresh sample (Fig. 1a) than on the aged one (Fig. 1b). The formation of reaction products can involve steps (5)–(7) over precious metal sites as illustrated in Scheme 1. Similar SP experiments performed at 400 °C (see Fig. 2) reveal the same trends on the outlet flow rates of NO than those previously observed at 450 °C. A fast response is followed by a long tail on the outlet NO flow rate curve recorded on the fresh Pd–Rh/Al_2O_3 ascribed to a spillover process of ad-NO_x species from the metal to the support. Interestingly, this long tail strongly attenuates on the aged sample. Based on these observations, fast and slow processes occur on the fresh catalyst related to reaction pathways involving only noble metals and the metal/support respectively. On the aged sample, the disappearance of the slow process seems in relative good agreement with the loss of metal dispersion from 0.31 to 0.21 as reported elsewhere [12] which reflects an alteration of the metal/support interface. Subsequent analyses of the evolution of N_2O selectivity on the aged Pd–Rh/Al_2O_3, at the beginning of the NO SP experiments during fast reaction pathways over noble metals, show a weak NO partial pressure dependency of the selectivity (Fig. 3). Similar behavior has been already reported essentially over rhodium based catalysts [14] at low temperature when the surface is quasi-completely covered by chemisorbed NO molecules. In these conditions, the residual N coverage is very low and the production of N_2 and N_2O would be predominantly governed by steps (6) and (7). In our operating temperature (T = 450 °C), only a small amount of NO is admitted during a SP experiment representing negligible coverage compared to the number of accessible sites. On the other hand, the surface is expected to be mostly covered by chemisorbed O atoms after stabilization which could induce the same selectivity behavior with strongly O chemisorbed atoms preventing the adsorption and the subsequent dissociation of chemisorbed NO molecules. Similar SP experiment performed at 400 °C (not shown) revealed the same selectivity behavior with N_2O selectivity insensitive to changes in NO concentration stabilizing at ≈0.94. Hence the shift observed on the selectivity from 0.94 to 0.73 with a rise in temperature would emphasize the fact that O desorption would govern the production of N_2O during NO SP experiments.
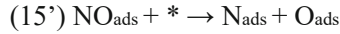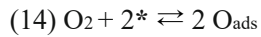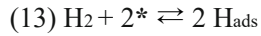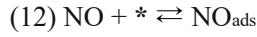
3.2 Steady-State Kinetic Model of the NO/H_2/O_2 Reaction on Aged Pd–Rh/Al_2O_3

Steady state rate measurements were performed under stoichiometric conditions on aged Pd–Rh/Al_2O_3 catalysts, pre-reduced in pure H_2 at 500 °C. The kinetics was investigated in the temperature range 60–85 °C with inlet partial pressures of NO, H_2 and O_2 varying in the range (0.7–1.2) x 10^{-3}, (2.0–4.0) x 10^{-3} and (0.5–1.5) x 10^{-3} atm. respectively. A significant decrease in the apparent activation energy value, from 106.8 to 84.9 kJ mol-1, is distinguishable on aged Pd–Rh/Al_2O_3 calculated from the slope of the Arrhenius plot in Fig. 4. Subsequent comparisons also show that this calculated value is intermediate between those previously obtained on freshly-prepared Pd–Rh/Al_2O_3 and Rh/Al_2O_3 catalysts [4].

Previous investigations on the kinetics of the NO/H_2 reaction on pre-reduced monometallic and bimetallic Pd–Rh [14, 15] were discussed on the basis of the mechanism Scheme 1 that differs from the nature of the dissociation step of NO assisted by the presence of chemisorbed hydrogen atoms (step (4)) or taking place on a nearest neighbor vacant site (step (4_0)). Previous experiments under lean and stoichiometric conditions showed that the competitive H_2/O_2 reaction may sometimes prevail inducing a strong depletion of the concentration of chemisorbed hydrogen. As a consequence, NO was found to dissociate predominantly on a nearest-neighbor vacant site [4]. On the other hand, a slow H_2/O_2 reaction and non-competitive adsorptions can induce a greater extent of H_{ads} at the vicinity of chemisorbed NO_{ads} that promotes subsequent NO dissociation in agreement with step (4). Regarding bimetallic catalysts, two borderline cases are currently envisioned as previously illustrated [16–18] that account for electronic and/or structural effects particularly for the removal of NO_x since NO dissociation step is currently considered as structure-sensitive [19]. Such effects may have some repercussions on the kinetic behavior if noble metals preserve their individual adsorptive properties in bimetallic particles or alternately if those ones are dramatically altered. In the former case, different affinity of Pd and Rh towards NO and H_2 adsorption would suggest preferential adsorptions as previously demonstrated on freshly-prepared Pd–Rh/Al_2O_3 [4]. Alternately, both metals can lose their individual properties due to subsequent electronic modifications that can originate peculiar catalytic

properties for the bimetallic Pt–Rh sites different from those characterizing the monometallic sites [17]. Both hypotheses have been considered for establishing a reaction rate expression that can model the partial pressure dependency of the rate on the aged sample.

As reported elsewhere [4], in case of non-competitive adsorptions, NO would be preferentially coordinated to Rh sites ($*_0$) and H_2 and O_2 to Pd sites ($*$) according to steps (12) and (13). For NO dissociation, the involvement of H_{ads} on Pd (step (15)) and/or a nearest neighbor Pd sites for the dissociation NO (step (15_0)) has been assumed. Thus, rate Eq. (16) can be derived which accounts for the following set of assumptions: (1) NO dissociation step as slow step— (2) fast adsorptions of the reactants at equilibrium—(3) chemisorbed H and O atoms and NO molecules as the most abundant species at the surface (Scheme 2).

(12) $NO + * \rightleftarrows NO_{ads}$

(13) $H_2 + 2* \rightleftarrows 2\,H_{ads}$

(14) $O_2 + 2* \rightleftarrows 2\,O_{ads}$

(15) $NO_{ads} + H_{ads} \rightarrow N_{ads} + OH_{ads}$

(15') $NO_{ads} + * \rightarrow N_{ads} + O_{ads}$

Scheme 2 Non-competitive adsorptions of NO and H_2 on Pd–Rh/Al_2O_3 [4]

$$r_1 = \frac{k_{15}\,K_{NO}P_{NO}\sqrt{K_{H_2}P_{H_2}}}{(1 + K_{NO}P_{NO})\left(1 + \sqrt{K_{H_2}P_{H_2}} + \sqrt{K_{O_2}P_{O_2}}\right)} + \frac{k_{15'}\,K_{NO}P_{NO}}{(1 + K_{NO}P_{NO})\left(1 + \sqrt{K_{H_2}P_{H_2}} + \sqrt{K_{O_2}P_{O_2}}\right)} \quad (16)$$

k_n et K_i are respectively the rate constant associated to step (n) and the equilibrium adsorption constant of the reactant i (i = NO, O_2 or H_2).

Now, in the case of competitive adsorptions of NO and H_2 on the aged Pd–Rh/Al_2O_3, Eq. (17) can be derived which accounts for the same assumptions and considering a dissociation of NO assisted by chemisorbed H atoms or taking place on a nearest neighbour vacant sites.

$$r_1 = \frac{k_4\,K_{NO}P_{NO}\sqrt{K_{H_2}P_{H_2}}}{\left(1 + K_{NO}P_{NO} + \sqrt{K_{H_2}P_{H_2}} + \sqrt{K_{O_2}P_{O_2}}\right)^2} + \frac{k_{4'}\,K_{NO}P_{NO}}{\left(1 + K_{NO}P_{NO} + \sqrt{K_{H_2}P_{H_2}} + \sqrt{K_{O_2}P_{O_2}}\right)^2} \quad (17)$$

k_n et K_i have been estimated from an adjustment routine with optimized parameters when the square difference between experimental and predicted rates using Eqs. (16) or (17) tends towards the lowest value as described elsewhere [20]. The residual sum of square reported in Table 1 does not provide decisive arguments to select the most appropriate Eqs. (16) or (17) for fitting experimental rate measurements. As observed the residual sum of square (RSS) values are comparable (see Table 1) with in both cases a good correlation between experimental and predicted rates. However, let us notice that the numerical value for NO adsorption constant is still much higher than those optimized for O_2 and H_2 adsorption. This observation combined with the weak NO partial pressure dependence on the selectivity still indicates that only rhodium is involved in the dissociation of NO and the formation of N_2O and N_2. This is in agreement with XPS measurements evidencing a significant surface Rh enrichment on the aged NGV catalysts [4].

3.3 N_2O Selectivity Behavior (TAP vs Steady-State Kinetic Measurements)

TAP and steady-state kinetic measurements where performed in different operating conditions i.e. pressure gap and temperature. Despite this fact, similar selectivity behaviour is observed which points out the importance of the stabilization prior to NO SP experiments. As mentioned, successive NO pulses till the stabilization of the conversion correspond to a pseudo steady-state where the surface of aged Pd–Rh/Al_2O_3 is mostly saturated by oxygen. Hence, the convergence observed on the selectivity

recorded at steady-state under atmospheric conditions would suggest comparable surface compositions during TAP experiments and steady-state kinetic measurements.

As demonstrated, S_{N_2O} depends on the rate $r_{N_2}=r_{N_2O}$ ratio. By examining Fig. 5, $r_{N_2}=r_{N_2O}$ varies as a function on the partial pressure of NO on single Pd/Al_2O_3 catalyst. On the contrary, it is clearly insensitive to change of the partial pressure of NO on Rh-based catalysts. Such a feature can be rationalised on the basis of the mechanism in Scheme 1.

$r_{N_2}=r_{N_2O}$ given by Eq. (18) depending on h_i and k_n related to step for the formation of N_2 and N_2O, can be calculated based on the steady-state approximation.

$$\frac{4\,r_{N_2}}{r_{N_2O}} + 1 = \frac{(k_6 + k_7)}{k_5}\left(\sqrt{1 + \frac{8k_5 k_{4\prime}\sqrt{K_H P_{H_2}}}{(k_6 + k_7)^2 K_{NO} P_{NO}}} + \frac{3k_6}{k_7}\right) \quad (18)$$

The weak partial pressure dependency of the N_2O-selectivity can be easily explained if the term $8k_5 k_{4\prime}\sqrt{K_H P_{H_2}}/(k_6 + k_7)^2 K_{NO} P_{NO}$ in Eq. (18) becomes negligible. Such a requirement is fulfilled when the numerical solutions for K_{NO}, k_6 and k_7 are significantly higher than the calculated values of K_H, k_5 and $k_{4\prime}$ which seems to be partly in agreement with data reported for K_{NO} and K_H in Table 1. Consequently, the simplification of Eq. (18) yielding Eq. (19) correctly explains the insensibility of selectivity to the partial pressure of NO.

$$\frac{r_{N_2}}{r_{N_2O}} \cong \frac{k_6}{k_7} \quad (19)$$

The value of $k_6/k_7 \approx 0.77$ on the aged Pd–Rh/Al_2O_3 catalyst can be roughly estimated from Fig. 5. The comparison with the value corresponding to the freshly-prepared catalyst emphasizes the detrimental effect of the thermal aging on the selectivity. Similarly, the constant selectivity around *0.73 recorded on the aged sample in very different conditions at 450 °C during NO SP experiment leads to a value of ≈ 0.3 which do not drastically differ from 0.77 taking the margin of error in this calculation.

All these considerations suggest that nitrosyl species would be less reactive towards NO dissociation on the aged sample.

4 Conclusion

The kinetics of NO adsorption and reaction with H_2 reaction have been studied from TAP and steady-state experiments. NO SP experiments at 450 °C where performed on aged Pd–Rh/Al_2O_3 previously submitted to successive NO pulses until to reach a state–state surface composition mostly populated by O-adsorbed atoms. As compared to a freshly-prepared catalyst, only a fast process is observed involving noble metals whereas the slow process associated to spill-over effect disappears. Steady-state rate measurements performed at much lower temperature 80 °C under atmospheric pressure were compared with two different mechanisms which essentially differ from the nature of the dissociation step of NO. While, no differentiation can be achieved kinetic data reflect the kinetic behavior of Rh consistently with a surface Rh enrichment induced by thermal aging. The high NO adsorption constant and the weak partial pressure dependency agree with active sites for NO transformation only composed of rhodium. Interestingly similar selectivity behavior is observed from TAP and steady-state rate measurements. The stabilization phase during successive NO pulses at 450 °C would play a key role leading to convergent surface adsorptive properties characterized from steady-state measurements.

References

1. Salaün M, Kouakou A, Da Costa A, Da Costa P (2009) Appl Catal B 88:386–397
2. Klingstedt F, Neyestanaki AK, Byggningsbacka R, Lindfors LE, Lundén M, Petersson M, Tengström P, Ollonqvist T, Väyrynen J (2001) Appl Catal A 209:301–316
3. Dhainaut F, Pietrzik S, Granger P (2007) Top Catal 42–43:135–141
4. Renème Y, Dhainaut F, Granger P (2012) Appl Catal B 111–112:424–432
5. Gelin P, Primet M (2009) Appl Catal B 39:1–37
6. Gremminger AT, Pereira de Carvalho HW, Popescu R, Grunwaldt JD, Deutshmann O (2015) Catal Today 258:277–284 doi:10.1016/j.cattod.2015.01.034
7. Granger P, Delannoy L, Leclercq L, Leclercq G (1998) J Catal 177:147–151
8. Granger P, Malfoy P, Leclercq L, Leclercq L (2004) J Catal 223:142–151
9. Granger P, Dhainaut F, Pietrzik S, Malfoy P, Mamede AS, Leclercq L, Leclercq G (2006) Top Catal 39:65–76
10. Hibbits DD, Jiménez R, Yoshimura M, Weiss B, Iglesia E (2014) J Catal 319:95–109
11. Frank B, Emig G, Renken A (1998) Appl Catal B 19:45–57
12. Renème Y, Dhainaut F, Schuurman Y, Mirodatos C, Granger P (2014) Appl Catal B 160–161:390–399
13. Gleaves JT, Yablonski GS, Phanawadee P, Schuurman Y (1997) Appl Catal A 160:55–88
14. Dhainaut F, Pietrzik S, Granger P (2008) J Catal 258:296–305
15. Dhainaut F, Pietrzik S, Granger P (2007) Appl Catal B 70:100–110
16. Ng KYS, Belton DN, Schmieg SJS, Fisher GB (1994) J Catal 146:394–406
17. Hu Z, Hallen FM, Wan CZ, Heck RM, Steger JJ, Lakis RE, Lyman CE (1998) J Catal 174:13–21
18. Granger P, Lecomte JJ, Dathy C, Leclercq L, Leclercq G (1998) J Catal 175:194–203
19. Peden CHF, Belton DN, Schmieg SJJ (1995) J Catal 155:204–218
20. Granger P, Lecomte JJ, Dathy C, Leclercq L, Leclercq G (1998) J Catal 173:304–31415